Research Square

Preprints are preliminary reports that have not undergone peer review.
They should not be considered conclusive, used to inform clinical practice,
or referenced by the media as validated information.

Backbone resonance assignment of the Human Heat Shock Protein B8 (HSPB8) across various denaturing conditions: A key to understanding its folding and function

Zainab Amin
Indian Institute of Science Education and Research (IISER)
Jeetender Chugh
cjeet@iiserpune.ac.in

Indian Institute of Science Education and Research (IISER)

Research Article

Keywords: Small Heat Shock Protein B8 (HSPB8), α-Crystallin Domain (ACD), Nuclear Magnetic Resonance (NMR) Spectroscopy, Backbone Resonance Assignment

Posted Date: June 25th, 2026

DOI: https://doi.org/10.21203/rs.3.rs-9968919/v1

License: This work is licensed under a Creative Commons Attribution 4.0 International License.
Read Full License

Additional Declarations: No competing interests reported.

Abstract

Heat shock protein B8 (HSPB8 or HSP22) is involved in key cellular processes, including cell migration, apoptosis, chromosomal segregation, and exhibits both pro-tumoral and anti-tumoral activities. Additionally, HSPB8 plays a crucial role in regulating cellular stress responses by stabilizing the misfolded proteins and preventing protein aggregation. Despite its biological importance, there are no comprehensive studies of HSPB8 at the molecular level as it forms dynamic oligomers in solution. Here, we address this gap by providing the sequence-specific backbone resonance assignments for the α-Crystallin Domain (ACD) of HSPB8 in the fully denatured state and along the folding path. We believe that this will serve as a foundation for future investigations into its functional conformation(s) crucial to the chaperone activity of HSPB8.

Biological context

Heat shock protein B8 (HSPB8 or HSP22) is a member of the small heat shock protein (sHSP) family of proteins characterized by their small molecular weight of ~ 12–43 kDa (Basha et al. 2012; Mogk et al. 2019). To date, 10 such proteins have been identified in humans (Kapp et al. 2003). The expression of sHSPs is regulated by the heat shock transcription factor (HSF) (Gomez-Pastor et al. 2018; Pessa et al. 2024; Smith and Mendillo 2026) and gets upregulated under the influence of different stressors (Haslbeck and Vierling 2015; Boelens 2020). The primary function of sHSPs is their chaperone or holdase activity, through which they bind and stabilize the early unfolding intermediates of its client proteins in an ATP-independent manner (Strauch and Haslbeck 2016; Collier and Benesch 2020; Reinle et al. 2022). This prevents protein aggregation and protect cells from proteotoxic stress, a key pathophysiology in protein misfolding disorders (Arrigo et al. 2002; Merendino et al. 2002; Ueom et al. 2003; Crippa et al. 2010b; Roman et al. 2017; Pessa et al. 2024). Under normal physiological conditions, sHSPs are stored as small, inactive oligomers. However, upon binding to substrates, these oligomers dissociate and assemble into larger, active complexes around the target proteins (Haslbeck and Vierling 2015; Mogk et al. 2019; Miller et al. 2023; Miller and Reichow 2024). Beyond their chaperone function, sHSPs are involved in several other cellular processes, including cell migration, apoptosis, cytoprotection, signaling, differentiation, and development (Xiong et al. 2020). Dysregulated expression and/or mutation(s) in these sHSPs have been associated with the pathogenesis of multiple diseases, such as cataracts, neurological disorders, myopathies, multiple sclerosis, aging, and cancers (Mymrikov et al. 2011; Ramírez-Rodríguez et al. 2013; Carra et al. 2017, 2019).

HSPB8 is ubiquitously expressed in vital tissues and organs of the human body, including skeletal and smooth muscles, spinal cord, motor and sensory neurons, heart, brain, prostate, lungs, and kidneys (Verschuure et al. 2003; Bouhy et al. 2018; Li et al. 2018). An increased expression of HSPB8 has been noted in different type of cancers (Yu et al. 2021). It is known to bind to proteins that are prone to misfolding, such as TDP-43 (TAR DNA-Binding Protein 43), c-Myc (Cellular Myelocytomatosis Oncogene), SOD1 (Superoxide Dismutase 1), etc. (Crippa et al. 2010a, 2016b, a; Chen et al. 2024). Apart from playing a crucial role in maintaining cellular homeostasis and chaperone activity, HSPB8 is integral to several

cellular pathways, including the protein quality control system – CASA (chaperone-assisted selective autophagy), protein degradation, and stress granule dynamism (Cristofani et al. 2021; Chierichetti et al. 2024; Du et al. 2024; Rashed et al. 2025). HSPB8 is also a crucial component of the cell division machinery, where it is involved in the accurate segregation of chromosomes and the orientation of the mitotic spindle (Fuchs et al. 2015; Varlet et al. 2017). In cellular context, its principle functional partners include BAG3 (BCL2-associated athanogene 3), HSP70 (Heat shock protein 70), CHIP / STUB1 (Carboxy-Terminus of HSC70-Interacting Protein / STIP1 Homology and U-Box Containing Protein 1), and p62 / SQSTM1 (Sequestosome 1) (Carra et al. 2008; Seidel et al. 2012). Previous studies have also shown the context-dependent pro-tumoral and anti-tumoral activities of this sHSP (Suzuki et al. 2015; Piccolella et al. 2017, 2021; Shi et al. 2018; Cristofani et al. 2021, 2022).

The full-length HSPB8 protein is 196 amino acids long (22 kDa) with a disordered long N-terminal region, a folded α-crystalline domain (ACD), flanked by another short-disordered C-terminal. As a conditionally disordered protein, HSPB8 can transition between highly ordered and less ordered conformations under different physiological conditions, which is essential for facilitating the proper folding of its client proteins (Rest et al. 2004; Fontaine et al. 2005). The ACD domain initiates the formation of the active oligomers by forming a dimeric building block with the help of intermolecular interactions (Carra et al. 2005; Haslbeck et al. 2005; Miller et al. 2023). These interactions are influenced by various internal and external stress conditions, thereby modulating the cellular activity of HSPB8 (Li et al. 2018). Despite the recognized biological significance of HSPB8, there is currently no comprehensive structural study focusing on HSPB8 or its ACD at a molecular level. In a recent study, we probed the effect of protein concentration, pH, and temperature on the monomer-dimer equilibrium of the ACD domain using NMR-based chemical shift perturbations and line broadening (Amin and Chugh 2025). Our studies predicted that the ACD domain has a predominantly β-enriched structure and forms a β7-interface dimer, based on the sequence homology with other members of the family (Haslbeck and Vierling 2015). We presumed that the chaperone function of HSPB8 may emerge from a spectrum of its own folding intermediates, which are distinct from the ordered native conformation. A knowledge gap about the deeper structural details exists that hinders our understanding of the precise mechanisms underlying the chaperone activity and folding processes of HSPB8. Therefore, understanding the structural features of these intermediates is essential for understanding the chaperone function of the protein at the molecular level. The current study aims to provide a first step to address this knowledge gap by providing the sequence specific backbone resonance assignment of the ACD of HSPB8 in different denaturant concentrations (urea concentrations from 8 M to 2 M). These assignments will serve as a critical foundation for future structural and conformational dynamics investigations, ultimately facilitating the characterization of folding intermediates and active conformations crucial to the chaperone activity of HSPB8.

Methods and Materials

Construct design

The cloning of the region encoding the ACD$^{74–185}$ (residues 74–185) into the pET28a vector was performed as described previously (Amin and Chugh 2025).

Sample preparation

The protein was purified as described elsewhere (Amin and Chugh 2025). Briefly, *Escherichia coli* cells overexpressing the HSPB8-ACD$^{74–185}$ were lysed using chemical lysis and sonication in a tris-based buffer (pH 7.5). The histidine (his)-tagged protein was isolated from the mixture of soluble proteins using Ni-NTA affinity chromatography. The $(His)_6$ tag was removed by incubating the eluate with TEV protease during overnight dialysis, followed by reverse Ni-NTA to remove free tag and the protease. A final purification was performed using size-exclusion chromatography. The purified protein was exchanged with phosphate-based buffer A (10 mM phosphate, 100 mM NaCl, 1 mM EDTA, and 1 mM DTT, pH 6.4) containing varied concentrations of urea (8, 6, 4, and 2 M, respectively).

Far-UV Circular Dichroism (CD) Spectroscopy

The purified protein sample (7 μM) in buffer A (without and with 8 M urea) was used to record far-UV CD spectra using the JASCO-815 series. The data was acquired from 260 to 200 nm in absence of urea and up to 210 nm in the presence of urea to avoid increased noise caused by the presence of urea. The spectra were recorded at a scanning speed of 50 nm/min and a bandwidth of 1 nm using a quartz cuvette with a 1 mm path length. The data has been represented as a mean of a total of 6 instrumental and 2 biological replicates after blank subtraction.

NMR Spectroscopy

All NMR experiments were recorded on an Ascend™ Bruker AVANCE III HD 14.1 Tesla (600 MHz) NMR spectrometer equipped with a quad-channel ($^{1}H/^{13}C/^{15}N/^{19}F$-$^{2}H$) cryoprobe. For resonance assignment, all NMR experiments were acquired at 298 K using a standard suite of double- and triple-resonance experiments, including ^{15}N-^{1}H HSQC, HNCA, HN(CO)CACB, HNCACB, HNCO, HNN, and ^{1}H-^{1}H TOCSY-HSQC (Sattler et al. 1999; Panchal et al. 2001; Shen et al. 2014). All spectra were acquired with Topspin (Bruker BioSpin) and referenced with respect to 2,2-dimethyl-2-silapentane-5-sulfonate (DSS), directly in the ^{1}H dimension and indirectly in the ^{15}N and ^{13}C dimensions (Wishart et al. 1995). The spectra were processed using TopSpin (Bruker BioSpin) and subsequently converted to UCSF format for analysis in POKY (Lee et al. 2021). The annotated HSQC figures were generated using POKY software.

Extent of assignment and data deposition

The full-length HSPB8 consists of 196 amino acids with a molecular weight of 22 kDa. In this study, a truncated construct from amino acids 74–185 was designed and used for NMR backbone assignment.

The truncated construct has three distinct regions: a disordered 22 amino acid long N-terminal region (residues 74–95), the conserved α-crystallin domain (ACD; residues 96–168), and 17 residues from the disordered C-terminal region (residues 169–185). After expression and $(His)_6$ tag cleavage, the overexpressed protein is left with 5 additional non-native residues (GGSEF) at the N-terminal making the working construct size of 117 residues. The backbone assignment of this protein was initially carried out in strongly denaturing conditions using 8 M urea, which helped in increasing the solubility and minimizing the conformational heterogeneity. Under these conditions, the protein adopted a predominantly unfolded state (Fig. 1A), facilitating efficient sequential resonance assignment using standard triple-resonance NMR experiments. Excluding the 13 proline residues, which lack amide protons, 101 out of the 104 expected backbone resonances (97% residues) were successfully assigned, including non-native residues (Fig. 1B). The primary sequence has been included for ready reference to highlight the residues (marked in grey) where assignments are not available (Fig. 1C).

To monitor the structural changes and maintain continuity of assignments during folding, the protein was subsequently dialyzed into low urea conditions of 6 M, 4 M, and 2 M. The assignment obtained in 8 M urea provided a reference dataset for subsequent assignment transfer during gradual refolding of the protein under these conditions. At each of these intermediate conditions, the backbone assignments were transferred and carefully validated using a combination of triple-resonance experiments (Fig. 2, 3, 4). This stepwise reduction in denaturant concentration enabled reliable tracking of resonance movements associated with conformational rearrangements and partial folding of the construct. The extent of assignment at each urea concentration has been summarized in Table 1. The progressive assignment strategy showed that several amino acids exhibited significant chemical shift changes as the urea concentration decreased, indicating changes in local structure during folding. Despite increased spectral overlap and line broadening under lower denaturant conditions, a substantial proportion of the backbone resonances could still be assigned. These assignments provide an important framework for investigating the folding behavior and conformational dynamics of the truncated HSPB8 construct under partially denaturing conditions.

All the assigned chemical shift data have been deposited in the Biological Magnetic Resonance Data Bank under the accession numbers 53814, 53815, 53816, and 53817, corresponding to samples in 8 M, 6 M, 4 M, and 2 M urea conditions, respectively, for the HSPB8-$ACD^{74–185}$. Additionally, the chemical shifts (backbone carbon and nitrogen, and all protons) at each urea condition were used to obtain secondary structure probabilities from the TALOS-N (Torsion Angle Likeliness Obtained from Shifts) server (Shen and Bax 2013, 2014). The secondary structure prediction by TALOS-N at 8 M urea was in close agreement with the AlphaFold-predicted structure (Fig. 5A). However, as the urea concentration was reduced (6 M, 4 M, 2 M), the secondary structure predictions became less accurate and showed poorer agreement with the AlphaFold-based secondary structure of the protein (Fig. 5B, 5C, 5D). We believe that at the lower urea concentrations, the protein may populate partially folded and heterogeneous intermediate states (Kjaergaard et al. 2010). This increased conformational heterogeneity causes

chemical shifts to deviate from both random-coil and well-defined native-state values, making ensemble-averaged chemical shifts less representative of a single structure (Rovó et al. 2013).

Declarations

Competing Interest Statement

The authors declare that they have no conflict of interest.

Funding

J.C. acknowledges extramural funding from the Science and Engineering Research Board (SERB), Govt. of India (EMR/2015/001966 and CRG/2023/002931-C), Department of Biotechnology (DBT), Govt. of India (BT/PR24185/BRB/10/1605/2017), Department of Health Research (DHR), ICMR (R.11015/14/2023-GIA/HR), and the generous intramural funding from IISER Pune. Z.A. thanks IISER Pune for the fellowship.

Author Contribution

J.C. and Z.A. conceived the study. Z.A. prepared and purified protein samples. Z.A. measured and analyzed all the NMR data. Z.A. prepare all the figures, J.C. edited all the figures, Z.A. and J.C. have both contributed toward manuscript writing.

Acknowledgement

The authors acknowledge April L. Darling and Vladimir N. Uversky (Department of Molecular Medicine, College of Medicine, Byrd Alzheimer's Institute, University of South Florida, Tampa, USA) for providing the FL-HSPB8 clone. The authors acknowledge the High-Field NMR facility at IISER-Pune (co-funded by DST-FIST and IISER Pune). Z.A. acknowledges Prof. Jayant B. Udgaonkar for providing access to the CD spectrometer and Biswajit Behera for assistance with the CD experiments.

Data Availability

The assignments for the HSPB8-ACD74-185 protein have been deposited in the BMRB under accession numbers 53814, 53815, 53816, and 58317 for 8 M, 6 M, 4 M, and 2 M urea conditions, respectively.

References

1. Amin Z, Chugh J (2025) NMR Insights Into Stress-Induced Modulation of the Monomer–Dimer Equilibrium in a Small Heat Shock Protein. Magn Reson Chem 63:1126–1136.

https://doi.org/10.1002/mrc.70042

2. Arrigo A-P, Paul C, Ducasse C et al (2002) Small Stress Proteins. Prog Mol Subcell Biol 28:171–184. https://doi.org/10.1007/978-3-642-56348-5_9
3. Basha E, O'Neill H, Vierling E (2012) Small heat shock proteins and α-crystallins: dynamic proteins with flexible functions. Trends Biochem Sci 37:106–117. https://doi.org/10.1016/j.tibs.2011.11.005
4. Boelens WC (2020) Structural aspects of the human small heat shock proteins related to their functional activities. Cell Stress Chaperones 25:581–591. https://doi.org/10.1007/s12192-020-01093-1
5. Bouhy D, Juneja M, Katona I et al (2018) A knock-in/knock-out mouse model of HSPB8-associated distal hereditary motor neuropathy and myopathy reveals toxic gain-of-function of mutant Hspb8. Acta Neuropathol 135:131–148. https://doi.org/10.1007/s00401-017-1756-0
6. Carra S, Alberti S, Arrigo PA et al (2017) The growing world of small heat shock proteins: from structure to functions. Cell Stress Chaperones 22:601–611. https://doi.org/10.1007/s12192-017-0787-8
7. Carra S, Alberti S, Benesch JLP et al (2019) Small heat shock proteins: multifaceted proteins with important implications for life. Cell Stress Chaperones 24:295–308. https://doi.org/10.1007/s12192-019-00979-z
8. Carra S, Seguin SJ, Lambert H, Landry J (2008) HspB8 Chaperone Activity toward Poly(Q)-containing Proteins Depends on Its Association with Bag3, a Stimulator of Macroautophagy*. J Biol Chem 283:1437–1444. https://doi.org/10.1074/jbc.m706304200
9. Carra S, Sivilotti M, Zobel ATC et al (2005) HspB8, a small heat shock protein mutated in human neuromuscular disorders, has in vivo chaperone activity in cultured cells. Hum Mol Genet 14:1659–1669. https://doi.org/10.1093/hmg/ddi174
10. Chen L, Wu M, Zhou Y (2024) HSPB8 binding to c-Myc alleviates hypoxia/reoxygenation-induced trophoblast cell dysfunction. Exp Ther Med 27:114. https://doi.org/10.3892/etm.2024.12402
11. Chierichetti M, Cristofani R, Crippa V et al (2024) Small heat shock protein B8: from cell functions to its involvement in diseases and potential therapeutic applications. Neural Regen Res 20:2872–2886. https://doi.org/10.4103/nrr.nrr-d-24-00517
12. Collier MP, Benesch JLP (2020) Small heat-shock proteins and their role in mechanical stress. Cell Stress Chaperones 25:601–613. https://doi.org/10.1007/s12192-020-01095-z
13. Crippa V, Carra S, Rusmini P et al (2010a) A role of small heat shock protein B8 (HspB8) in the autophagic removal of misfolded proteins responsible for neurodegenerative diseases. Autophagy 6:958–960. https://doi.org/10.4161/auto.6.7.13042
14. Crippa V, Cicardi ME, Ramesh N et al (2016a) The chaperone HSPB8 reduces the accumulation of truncated TDP-43 species in cells and protects against TDP-43-mediated toxicity. Hum Mol Genet 25:3908–3924. https://doi.org/10.1093/hmg/ddw232
15. Crippa V, D'Agostino VG, Cristofani R et al (2016b) Transcriptional induction of the heat shock protein B8 mediates the clearance of misfolded proteins responsible for motor neuron diseases. Sci

Rep 6:22827. https://doi.org/10.1038/srep22827

16. Crippa V, Sau D, Rusmini P et al (2010b) The small heat shock protein B8 (HspB8) promotes autophagic removal of misfolded proteins involved in amyotrophic lateral sclerosis (ALS). Hum Mol Genet 19:3440–3456. https://doi.org/10.1093/hmg/ddq257
17. Cristofani R, Piccolella M, Crippa V et al (2021) The Role of HSPB8, a Component of the Chaperone-Assisted Selective Autophagy Machinery, in Cancer. Cells 10:335. https://doi.org/10.3390/cells10020335
18. Cristofani R, Piccolella M, Marelli MM et al (2022) HSPB8 counteracts tumor activity of BRAF- and NRAS-mutant melanoma cells by modulation of RAS-prenylation and autophagy. Cell Death Dis 13:973. https://doi.org/10.1038/s41419-022-05365-9
19. Du W, Guo K, Wang P et al (2024) HSPB8 Facilitates the Oncogenesis and Advancement of Bladder Cancer via Activation of HSP27. J Cancer 15:645–658. https://doi.org/10.7150/jca.89994
20. Fontaine J-M, Sun X, Benndorf R, Welsh MJ (2005) Interactions of HSP22 (HSPB8) with HSP20, αB-crystallin, and HSPB3. Biochem Biophys Res Commun 337:1006–1011. https://doi.org/10.1016/j.bbrc.2005.09.148
21. Fuchs M, Luthold C, Guilbert SM et al (2015) A Role for the Chaperone Complex BAG3-HSPB8 in Actin Dynamics, Spindle Orientation and Proper Chromosome Segregation during Mitosis. PLoS Genet 11:e1005582. https://doi.org/10.1371/journal.pgen.1005582
22. Gomez-Pastor R, Burchfiel ET, Thiele DJ (2018) Regulation of heat shock transcription factors and their roles in physiology and disease. Nat Rev Mol Cell Biol 19:4–19. https://doi.org/10.1038/nrm.2017.73
23. Haslbeck M, Franzmann T, Weinfurtner D, Buchner J (2005) Some like it hot: the structure and function of small heat-shock proteins. Nat Struct Mol Biol 12:842–846. https://doi.org/10.1038/nsmb993
24. Haslbeck M, Vierling E (2015) A First Line of Stress Defense: Small Heat Shock Proteins and Their Function in Protein Homeostasis. J Mol Biol 427:1537–1548. https://doi.org/10.1016/j.jmb.2015.02.002
25. Kapp G, Franck E, Verschuure P et al (2003) The human genome encodes 10 -crystallinrelated small heat shock proteins: HspB110. Cell Stress Chaperones 8:53–61. https://doi.org/10.1379/1466-1268(2003)8%3C53:thgecs%3E2.0.co;2
26. Kjaergaard M, Teilum K, Poulsen FM (2010) Conformational selection in the molten globule state of the nuclear coactivator binding domain of CBP. Proc Natl Acad Sci 107:12535–12540. https://doi.org/10.1073/pnas.1001693107
27. Lee W, Rahimi M, Lee Y, Chiu A (2021) POKY: a software suite for multidimensional NMR and 3D structure calculation of biomolecules. Bioinformatics 37:3041–3042. https://doi.org/10.1093/bioinformatics/btab180
28. Li F, Xiao H, Hu Z et al (2018) Exploring the multifaceted roles of heat shock protein B8 (HSPB8) in diseases. Eur J Cell Biol 97:216–229. https://doi.org/10.1016/j.ejcb.2018.03.003

29. Merendino AM, Paul C, Vignola AM et al (2002) Heat shock protein-27 protects human bronchial epithelial cells against oxidative stressmediated apoptosis: possible implication in asthma. Cell Stress Chaperones 7:269–280. https://doi.org/10.1379/1466-1268(2002)007%3C0269:hspphb%3E2.0.co;2
30. Miller AP, O'Neill SE, Lampi KJ, Reichow SL (2023) The α-crystallin chaperones undergo a quasi-ordered co-aggregation process in response to saturating client interaction. bioRxiv 2023.08.15.553435 https://doi.org/10.1101/2023.08.15.553435
31. Miller AP, Reichow SL (2024) Mechanism of small heat shock protein client sequestration and induced polydispersity. bioRxiv 2024.12.03.626640. https://doi.org/10.1101/2024.12.03.626640
32. Mogk A, Ruger-Herreros C, Bukau B (2019) Cellular Functions and Mechanisms of Action of Small Heat Shock Proteins. Annu Rev Microbiol 73:1–22. https://doi.org/10.1146/annurev-micro-020518-115515
33. Mymrikov EV, Seit-Nebi AS, Gusev NB (2011) Large Potentials of Small Heat Shock Proteins. Physiol Rev 91:1123–1159. https://doi.org/10.1152/physrev.00023.2010
34. Panchal SC, Bhavesh NS, Hosur RV (2001) Improved 3D triple resonance experiments, HNN and HN(C)N, for HN and 15N sequential correlations in (13C, 15N) labeled proteins: Application to unfolded proteins. J Biomol NMR 20:135–147. https://doi.org/10.1023/a:1011239023422
35. Pessa JC, Joutsen J, Sistonen L (2024) Transcriptional reprogramming at the intersection of the heat shock response and proteostasis. Mol Cell 84:80–93. https://doi.org/10.1016/j.molcel.2023.11.024
36. Piccolella M, Crippa V, Cristofani R et al (2017) The small heat shock protein B8 (HSPB8) modulates proliferation and migration of breast cancer cells. Oncotarget 8:10400–10415. https://doi.org/10.18632/oncotarget.14422
37. Piccolella M, Cristofani R, Tedesco B et al (2021) Retinoic Acid Downregulates HSPB8 Gene Expression in Human Breast Cancer Cells MCF-7. Front Oncol 11:652085. https://doi.org/10.3389/fonc.2021.652085
38. Ramírez-Rodríguez G, Babu H, Klempin F et al (2013) The α Crystallin Domain of Small Heat Shock Protein b8 (Hspb8) Acts as Survival and Differentiation Factor in Adult Hippocampal Neurogenesis. J Neurosci 33:5785–5796. https://doi.org/10.1523/jneurosci.6452-11.2013
39. Rashed HR, Nath SR, Milone M (2025) The Spectrum of Small Heat Shock Protein B8 (HSPB8)-Associated Neuromuscular Disorders. Int J Mol Sci 26:2905. https://doi.org/10.3390/ijms26072905
40. Reinle K, Mogk A, Bukau B (2022) The Diverse Functions of Small Heat Shock Proteins in the Proteostasis Network. J Mol Biol 434:167157. https://doi.org/10.1016/j.jmb.2021.167157
41. Rest JS, Sun X, Fontaine J-M et al (2004) Interaction of Human HSP22 (HSPB8) with Other Small Heat Shock Proteins*. J Biol Chem 279:2394–2402. https://doi.org/10.1074/jbc.m311324200
42. Roman SG, Chebotareva NA, Kurganov BI (2017) Anti-aggregation activity of small heat shock proteins under crowded conditions. Int J Biol Macromol 100:97–103. https://doi.org/10.1016/j.ijbiomac.2016.05.080

43. Rovó P, Stráner P, Láng A et al (2013) Structural Insights into the Trp-Cage Folding Intermediate Formation. Chem Eur J 19:2628–2640. https://doi.org/10.1002/chem.201203764
44. Sattler M, Schleucher J, Griesinger C (1999) Heteronuclear multidimensional NMR experiments for the structure determination of proteins in solution employing pulsed field gradients. Prog Nucl Magn Reson Spectrosc 34:93–158. https://doi.org/10.1016/s0079-6565(98)00025-9
45. Seidel K, Vinet J, Dunnen WFA et al (2012) den, The HSPB8-BAG3 chaperone complex is upregulated in astrocytes in the human brain affected by protein aggregation diseases. Neuropathol Appl Neurobiol 38:39–53. https://doi.org/10.1111/j.1365-2990.2011.01198.x
46. Shen M, Trébosc J, Lafon O et al (2014) Improving the resolution in proton-detected through-space heteronuclear multiple quantum correlation NMR spectroscopy. J Magn Reson 245:38–49. https://doi.org/10.1016/j.jmr.2014.05.006
47. Shen Y, Bax A (2013) Protein backbone and sidechain torsion angles predicted from NMR chemical shifts using artificial neural networks. J Biomol NMR 56:227–241. https://doi.org/10.1007/s10858-013-9741-y
48. Shen Y, Bax A (2014) Artificial Neural Networks. Methods Mol Biol 1260:17–32. https://doi.org/10.1007/978-1-4939-2239-0_2
49. Shi J, Chen S, Guo C et al (2018) The mTOR inhibitor AZD8055 overcomes tamoxifen resistance in breast cancer cells by down-regulating HSPB8. Acta Pharmacol Sin 39:1338–1346. https://doi.org/10.1038/aps.2017.181
50. Smith RS, Mendillo ML (2026) Heat shock transcription factors in development and disease. Dis Model Mech 19:dmm052700. https://doi.org/10.1242/dmm.052700
51. Strauch A, Haslbeck M (2016) The function of small heat-shock proteins and their implication in proteostasis. Essays Biochem 60:163–172. https://doi.org/10.1042/ebc20160010
52. Suzuki M, Matsushima-Nishiwaki R, Kuroyanagi G et al (2015) Regulation by heat shock protein 22 (HSPB8) of transforming growth factor-α-induced ovary cancer cell migration. Arch Biochem Biophys 571:40–49. https://doi.org/10.1016/j.abb.2015.02.030
53. Ueom J, Kwon S, Kim S et al (2003) Acquisition of heat shock tolerance by regulation of intracellular redox states. Biochim Biophys Acta (BBA) -. Mol Cell Res 1642:9–16. https://doi.org/10.1016/s0167-4889(03)00081-8
54. Varlet AA, Fuchs M, Luthold C et al (2017) Fine-tuning of actin dynamics by the HSPB8-BAG3 chaperone complex facilitates cytokinesis and contributes to its impact on cell division. Cell Stress Chaperones 22:553–567. https://doi.org/10.1007/s12192-017-0780-2
55. Verschuure P, Tatard C, Boelens WC et al (2003) Expression of small heat shock proteins HspB2, HspB8, Hsp20 and cvHsp in different tissues of the perinatal developing pig. Eur J Cell Biol 82:523–530. https://doi.org/10.1078/0171-9335-00337
56. Wishart DS, Bigam CG, Yao J et al (1995) 1H, 13C and 15N chemical shift referencing in biomolecular NMR. J Biomol Nmr 6:135–140. https://doi.org/10.1007/bf00211777

57. Xiong J, Li Y, Tan X, Fu L (2020) Small Heat Shock Proteins in Cancers: Functions and Therapeutic Potential for Cancer Therapy. Int J Mol Sci 21:6611. https://doi.org/10.3390/ijms21186611
58. Yu L-L, Wang Y, Xiao Z-K, Chen S-S (2021) Heat shock protein B8 promotes proliferation and migration in lung adenocarcinoma A549 cells by maintaining mitochondrial function. Mol Cell Biochem 476:187–197. https://doi.org/10.1007/s11010-020-03896-3

Table

Table 1
The percentage of nitrogen (^{15}N), carbon ($^{13}C_{\alpha}$, $^{13}C_{\beta}$, ^{13}CO), and proton (^{1}H including amide and side-chain protons) backbone assignments of HSPB8-ACD$^{74–185}$ at different urea concentrations.

S. No.	Condition	^{15}N (%)	$^{13}C_{\alpha}$ (%)	$^{13}C_{\beta}$ (%)	^{13}CO (%)	^{1}H (%)
1	8 M Urea	84.6	84.6	85.7	82	72.9
2	6 M Urea	85.4	85.4	85.7	85.4	83.6
3	4 M Urea	85.4	85.4	85.7	85.4	82.3
4	2 M Urea	78.6	78.6	78	78.6	75.4

Figures

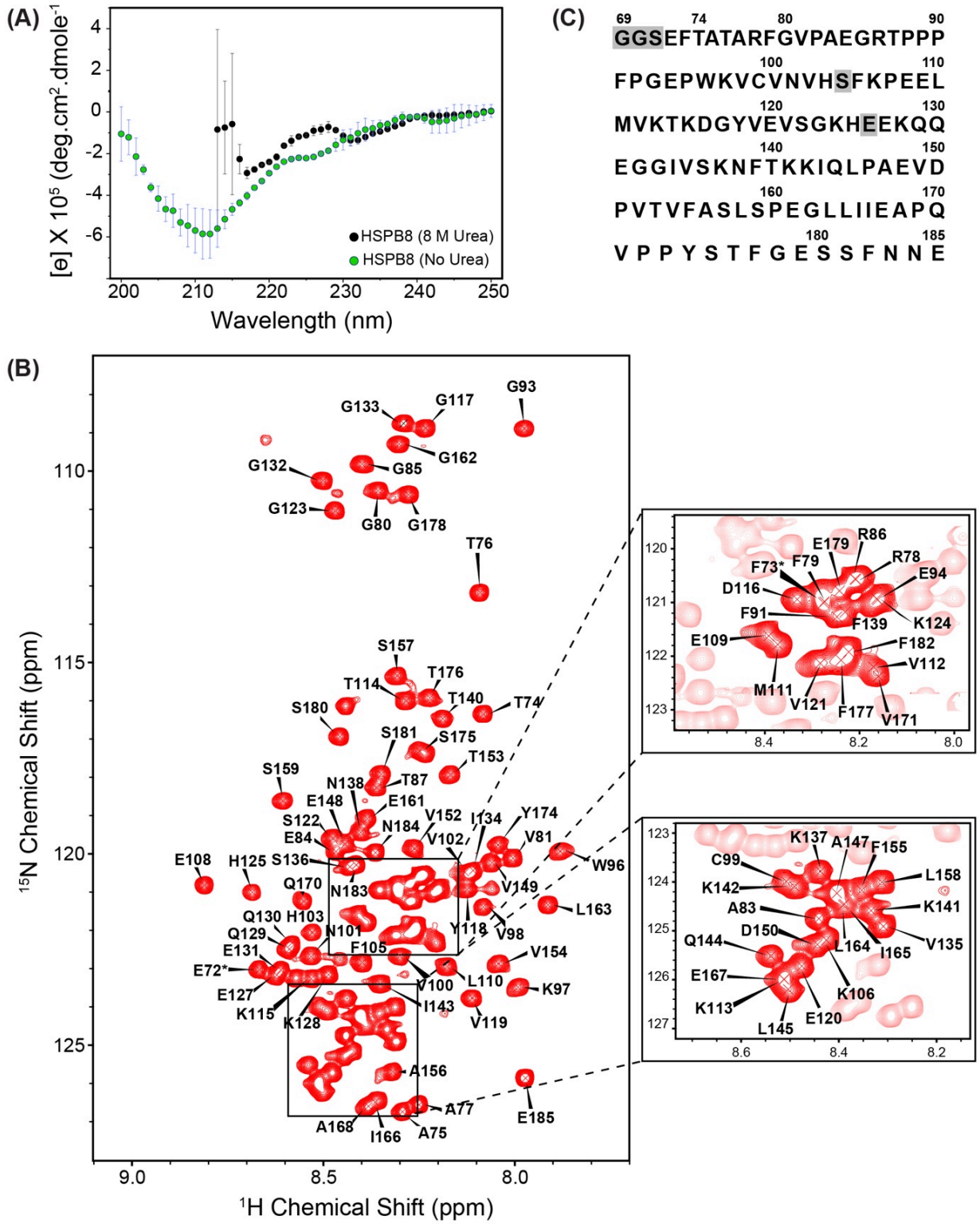


Figure 1

(A) An overlay of far-UV circular dichroism (CD) spectrum of the HSPB8-ACD$^{74\text{-}185}$ protein in the presence (black) and absence of 8 M urea (green). The CD spectrum recorded in the presence of 8 M urea (green) shows a loss of native secondary structure due to strongly denaturing conditions, indicating that the protein is unfolded. **(B)** 2D ^{15}N-^{1}H HSQC of HSPB8-ACD$^{74\text{-}185}$ in 8 M urea. Each peak has been labeled with the respective amino acid (one letter code) and residue number. The non-native residues

(GGSEF) present at the N-terminal have been numbered with a star. The crowded areas have been zoomed for clarity in the inset. (**C**) The primary amino acid sequence, where the unassigned amino acids have been highlighted in grey.

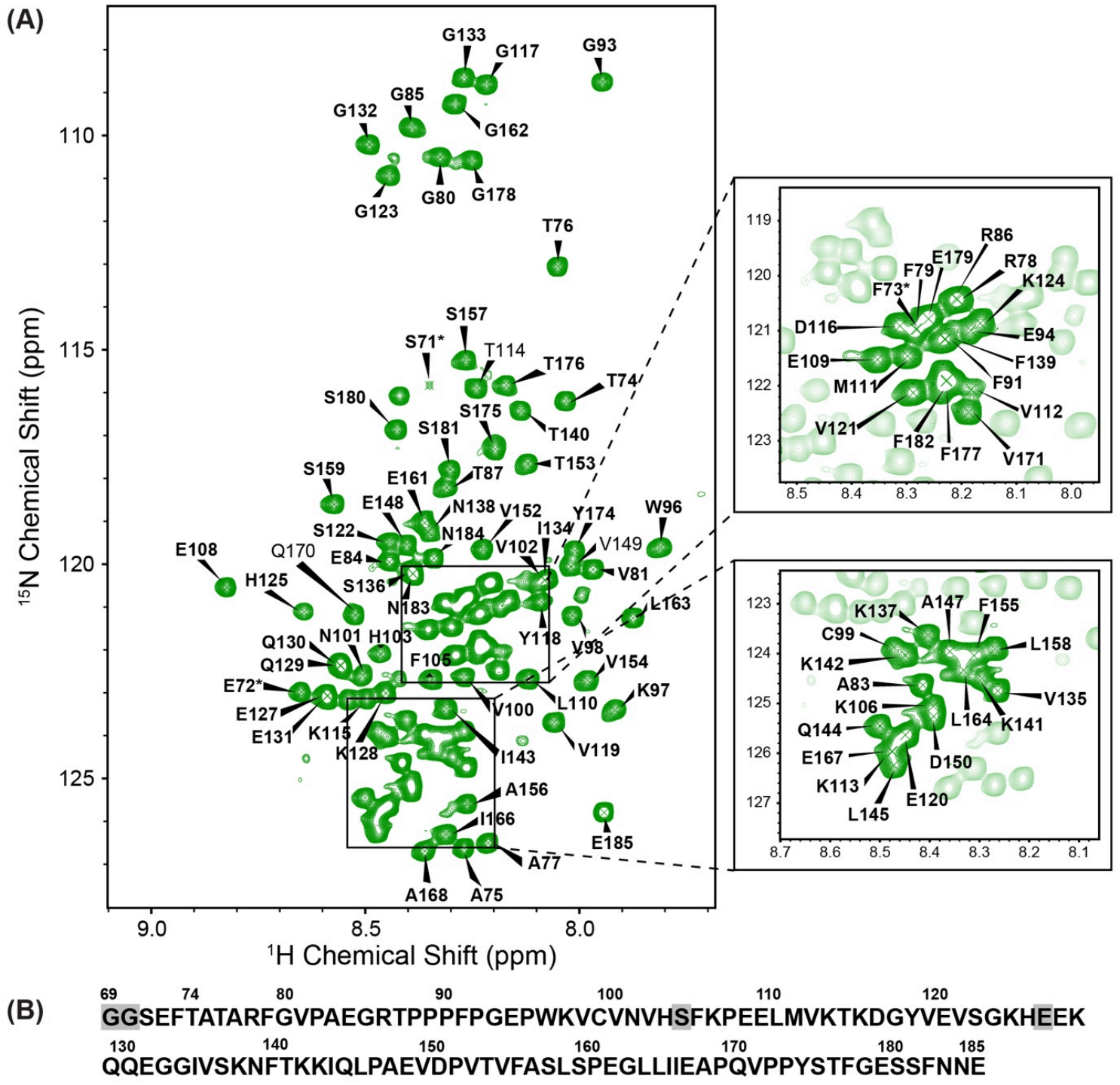


Figure 2

(**A**) 2D ^{15}N-^{1}H HSQC of the HSPB8-ACD$^{74\text{-}185}$ in the presence of 6 M urea. Each peak has been labeled with the respective amino acid (one letter code) and residue number. The non-native residues (GGSEF) present at the N-terminal have been numbered with a star. The crowded areas have been highlighted

separately in the inset. (**B**) The primary amino acid sequence, where the unassigned amino acids have been highlighted in grey.

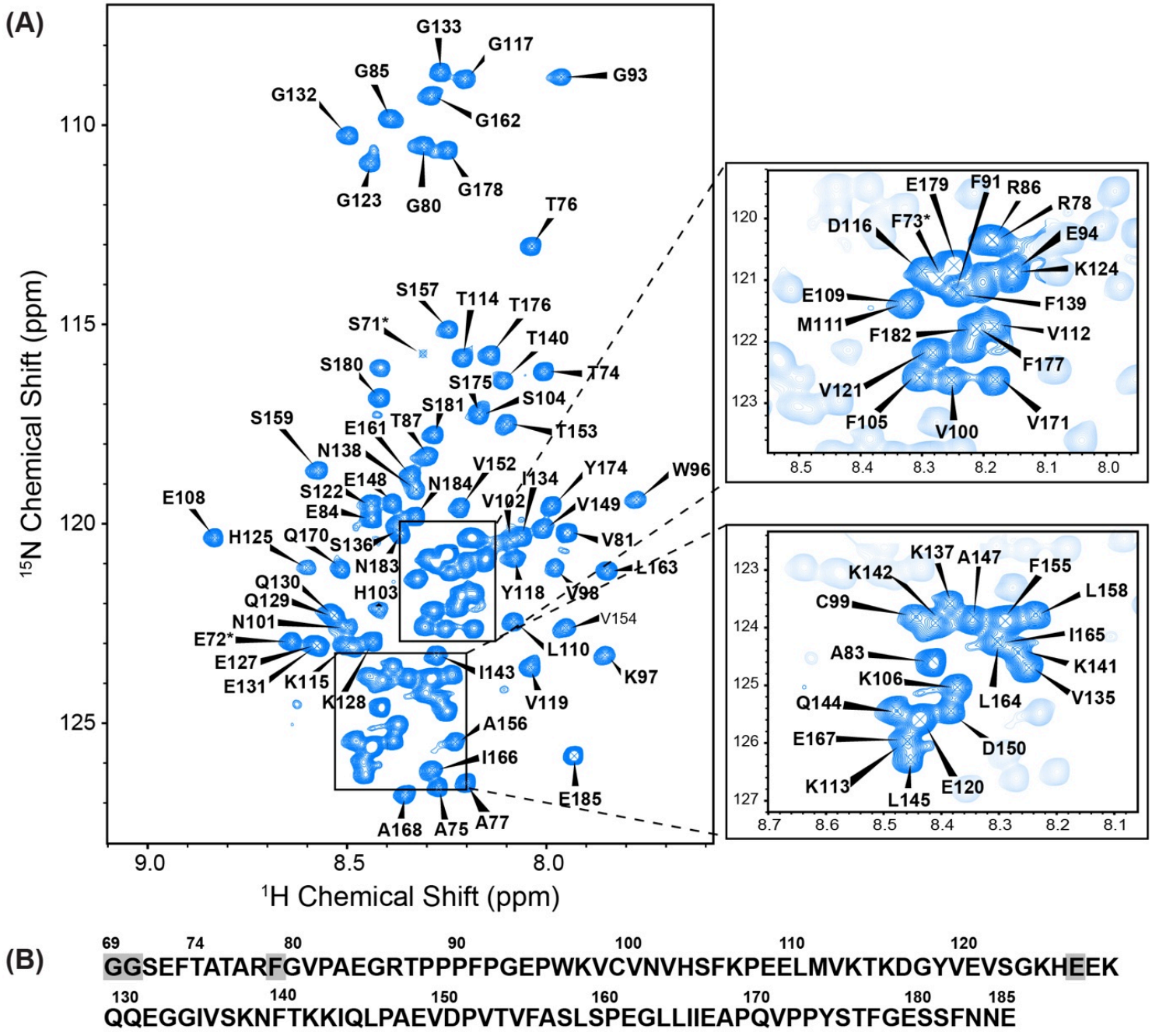


Figure 3

(**A**) 2D ^{15}N-^{1}H HSQC of the HSPB8-ACD$^{74-185}$ in the presence of 4 M urea. Each peak has been labeled with the respective amino acid (one letter code) and residue number. The non-native residues (GGSEF) present at the N-terminal have been numbered with a star. The crowded areas have been highlighted separately in the inset. (**B**) The primary amino acid sequence, where the unassigned amino acids have been highlighted in grey.

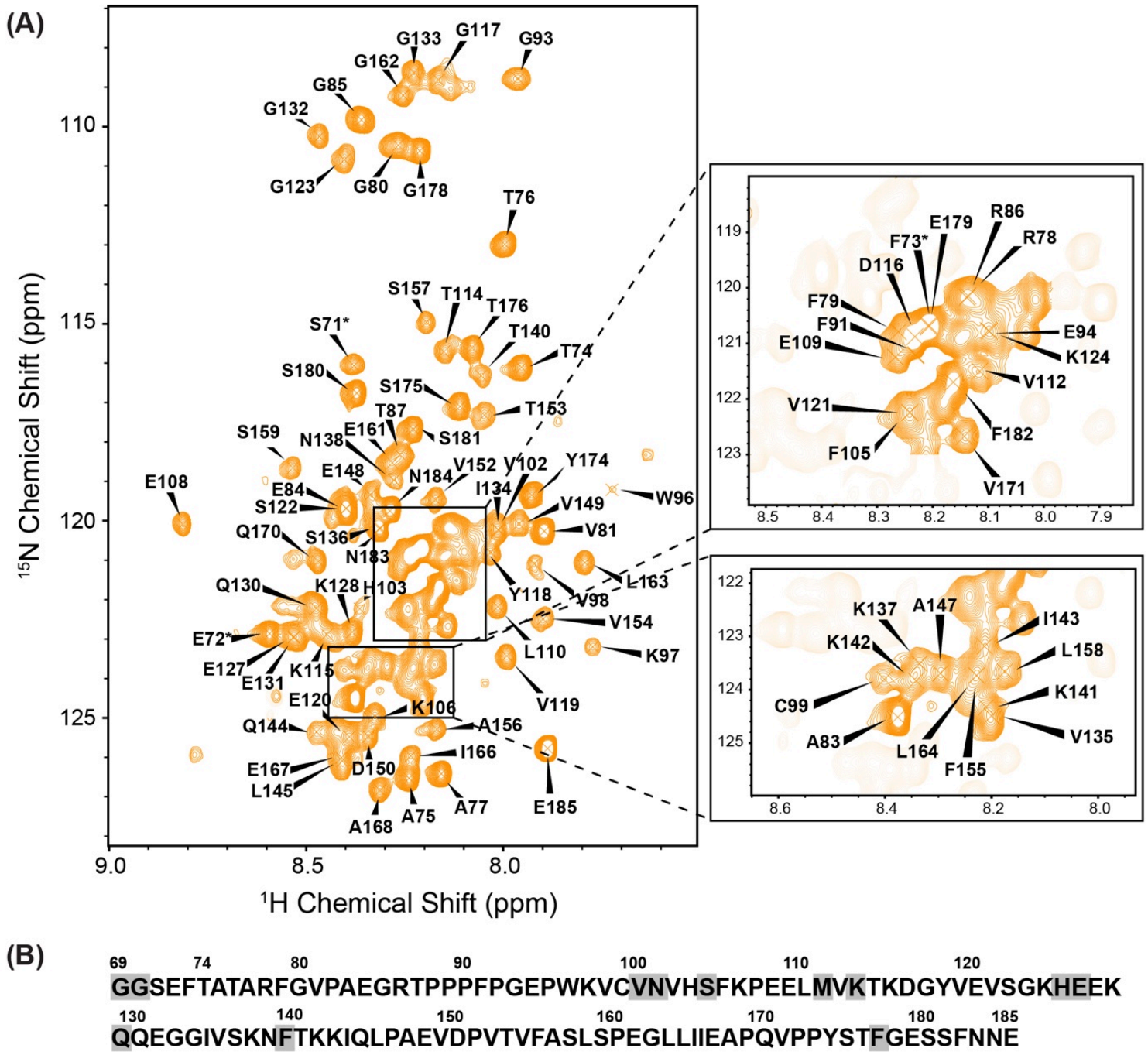


Figure 4

(**A**) 2D ^{15}N-^{1}H HSQC of the HSPB8-ACD$^{74-185}$ in the presence of 2 M urea. Each peak has been labeled with the respective amino acid (one letter code) and residue number. The non-native residues (GGSEF) present at the N-terminal have been numbered with a star. The crowded areas have been highlighted separately in the inset. (**B**) The primary amino acid sequence, where the unassigned amino acids have been highlighted in grey.

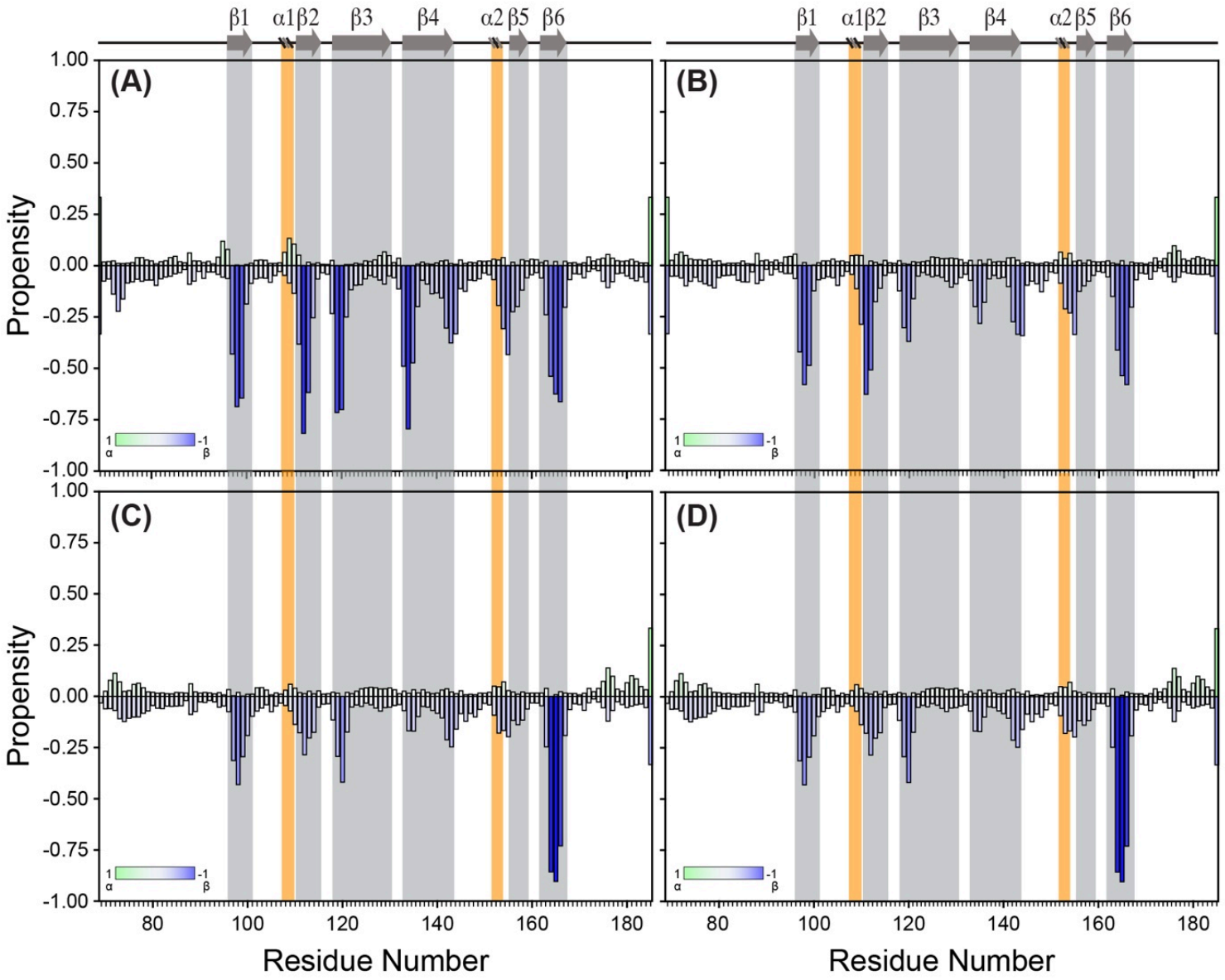


Figure 5

The secondary structure predictions of the HSPB8-ACD$^{74\text{-}185}$ protein at different urea concentrations using TALOS-N plotted against residue numbers. The secondary structure probabilities were derived from NMR chemical shifts using TALOS-N at **(A)** 8 M, **(B)** 6 M, **(C)** 4 M, and **(D)** 2 M urea, respectively. The orange and grey lines depict the secondary structures (α-helices and β-sheets, respectively), as predicted by the AlphaFold model for comparison.